Journal of Pharmaceutical Analysis 10 (2020) 346–350

Contents lists available at ScienceDirect

Journal of Pharmaceutical Analysis

journal homepage: www.elsevier.com/locate/jpa

Original article

Identification of impurities in nafamostat mesylate using HPLC-IT-TOF/MS: A series of double-charged ions

Yuxin Zhang [a], Lufan An [b], Lin Zhang [c], Rulin Wang [d], Yuan Tian [d], Zunjian Zhang [d, *]

[a] Nanjing Drum Tower Hospital, The Affiliated Hospital of Nanjing University Medical School, Nanjing, 210008, PR China
[b] Jiangsu D&R Pharmaceutical Corporation, Taizhou, 225312, PR China
[c] Department of Pharmacy, General Hospital Tianjin Medical University, Tianjin, 300052, PR China
[d] Key Laboratory of Drug Quality Control and Pharmacovigilance (Ministry of Education), China Pharmaceutical University, Nanjing, 210009, PR China

ARTICLE INFO

Article history:
Received 8 July 2019
Received in revised form
24 February 2020
Accepted 1 March 2020
Available online 3 March 2020

Keywords:
Nafamostat mesylate
Impurity
Structure identification
Double-charged ion

ABSTRACT

Nafamostat mesylate is a serine protease inhibitor used in the treatment of acute pancreatitis. The impurities in nafamostat mesylate, the active pharmaceutical ingredient (API), were profiled via high performance liquid chromatography tandem ion trap coupled with time-of-flight mass spectrometer (HPLC-IT-TOF/MS). The chromatography was performed on an ACE-3 C_{18} column (200 mm × 4.6 mm, 3 μm) using methanol and 0.1% formic acid in purified water as mobile phase at a flow rate of 1.0 mL/min. The ions were detected by IT-TOF/MS with a full-scan mass analysis from *m/z* 100 to 800. In total, eleven impurities were detected in nafamostat mesylate API. The impurity profile was estimated based on the HPLC-IT-TOF/MS data, including accurate masses, MS^n fingerprints of fragmentation pathways and a series of double-charged ions. Finally, seven impurities were identified and reported for the first time. The results will provide technical support for the quality control and clinical safety of nafamostat mesylate.

1. Introduction

Nafamostat mesylate (benzoic acid, 4-[(aminoiminomethyl) amino]-, 6-(aminoimino-methyl)-2-naphthalenyl ester, dimethanesulfonate; CAS: 82956-11-4, Fig. 1) is a serine protease inhibitor used in the treatment of acute pancreatitis and disseminated intravascular coagulation [1–6]. It can effectively prevent post-endoscopic retrograde cholangiopancreatography pancreatitis [7]. As an anticoagulant in continuous hemofiltration and continuous hemodiafiltration, it has shown efficacy in critically ill patients [8]. It is reported that nafamostat mesylate is effective for proteinuria and hypocomplementemia in the treatment of systemic lupus erythematosus with nephrotic syndrome [9]. Dose-dependent cardio-protection was observed, which demonstrates that nafamostat can reduce inflammatory myocardial injury by complement and neutrophil inhibition [10].

Several methods have been reported, including high performance liquid chromophotograph coupled with an ultraviolet detector (HPLC-UV) [11] and solid-phase extraction mass spectrometry (SPE-MS) [12] to determine nafamostat mesylate as a single analyte [12], in combination with its important metabolites [11], with other drugs in vitro, or in biological samples [4,6]. However, a systematic method for detecting and identifying the impurity profile in nafamostat mesylate is not available and it is necessary to develop one.

In this work, a rapid HPLC-IT-TOF/MS-based method was developed to profile the impurities in nafamostat mesylate. Eleven impurities were detected by it. The fragmentation pathways of the nafamostat mesylate API were interpreted through accurate measurements of *m/z* values combined with MS^n fragmentation analysis. A series of double-charged ions were detected. According to their fragmentation pathways, seven impurities were identified for the first time, which will help improve the quality control and clinical safety of nafamostat mesylate.

2. Materials and methods

2.1. Chemicals, reagents and materials

The three batches of nafamostat mesylate active pharmaceutical

Peer review under responsibility of Xi'an Jiaotong University.
* Corresponding author.
E-mail address: zunjianzhangcpu@hotmail.com (Z. Zhang).

https://doi.org/10.1016/j.jpha.2020.03.002

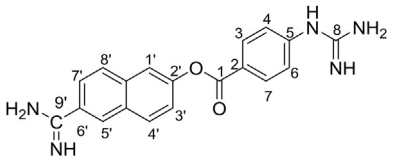

Fig. 1. Structure of nafamostat.

ingredient (Batch No.s:14092001, 14092002, 14092003) were supplied by Jiangsu D&R Pharmaceutical Corporation (Taizhou, P. R. China). Methanol of chromatographic grade was purchased from Merck (Merck Company, Germany). Formic acid was of analytical grade and purchased from Nanjing Chemical Reagent Co., Ltd. (Nanjing, P. R. China). Double distilled water was prepared by passing water through the Milli-Q Water System (Merck Millipore, Massachusetts, USA).

2.2. Instrumentation

The chromatographic separation was performed on a Shimadzu UFLC system (Shimadzu, Kyoto, Japan). The LC system consists of an LC-30AD pump system, an SIL-30AC autosampler, a CTO-20AC column oven, a CBM-20 Alite system controller, an SDPM20A diode array detector and a hybrid ion trap/time-of-flight mass spectrometer (IT-TOF/MS, Shimadzu, Kyoto, Japan), controlled by LCMS solution software (version 3.0, Shimadzu).

2.3. Chromatographic conditions

The chromatography was carried out on an ACE-3 C_{18} column (200 mm × 4.6 mm, 3 μm) using methanol (A) and 0.1% formic acid in purified water (B). A gradient elution was adopted, starting with 23% A, and was linearly increased to 30% A at 3 min, 35% A at 5 min, 40% A at 7 min, and maintained with 40% A until 12 min and with 55% A from 12th to 20th min. The column temperature was kept at 40 °C. The flow rate was 1.0 mL/min. The samples (20 μL) were injected into the HPLC-IT-TOF/MS with a split ratio of 5:1 (*V/V*).

2.4. Mass spectrometry

The electrospray ionization (ESI) source was set at both positive and negative ionization modes. Ultra-high-purity Ar was used as the collision gas and high-purity N_2 as the nebulizing gas at a flow rate of 1.5 mL/min. The MS instrumental parameters were set as follows: The curved desorption line (CDL) and heat block temperatures were both 200 °C. The interface voltage was set at 4.5 kV for the positive mode and −3.5 kV for the negative mode, and the detector voltage at 1.65 kV. The scanned mass range was from *m/z* 100 to *m/z* 800 using an accumulation time of 20 ms per spectrum. The mass spectrometry was calibrated with the standard calibration solution before sample analysis. The mass deviation of the instrument was within 10 ppm.

2.5. Sample preparation

Standard stock solutions for three batches of nafamostat mesylate were prepared at a concentration of 4 mg/mL. Approximately 40 mg of nafamostat mesylate API was transferred to a 10 mL volumetric flask and dissolved in 10 mL water. Then the standard stock solution was stored at 4 °C before the HPLC-IT-TOF/MS analysis.

3. Results and discussion

A rapid approach using HPLC-IT-TOF/MS was developed to detect and identify the impurities in nafamostat mesylate. After detection, the characteristic product ions and fragmentation pathways were interpreted. The structures of the impurities were identified from the MS^n fingerprints of fragmentation pathways by comparing those of the impurities and that of the active pharmaceutical ingredient. The workflow is summarized in Fig. 2.

3.1. HPLC conditions and sample preparation

Several previous reports that determined nafamostat mesylate used non-volatile phase buffers, which are incompatible with MS analysis. To overcome this limitation, a mobile phase of volatile formic acid was used. To obtain chromatograms with good resolution for nafamostat mesylate and its impurities, the HPLC conditions were established by testing different mobile phases. Different proportions of methanol or acetonitrile with different concentrations of formic acid were tested to separate the API and its impurities. The results indicated that methanol gave better resolution than acetonitrile. However, neither one of them could completely separate nafamostat mesylate and its impurities in isocratic elution. In the end, a gradient elution was chosen with a mobile phase consisting of methanol and 0.1% formic acid in purified water.

3.2. HPLC analysis

The chromatograms of nafamostat mesylate are shown in Fig. 3. Eleven impurities were detected in all three batches of the API through the developed method, and seven of them, i.e., impurities **A**, **B**, **D**, **E**, **F**, **H** and **I**, were ultimately identified.

3.3. Fragmentation pathways of nafamostat mesylate

It is necessary to understand the fragmentation pathways of nafamostat mesylate in order to identify its impurities. Characteristic MS^n fingerprint product ions were detected. Table 1 shows *m/z* values and mass differences between values observed by IT-TOF/MS and calculated. Due to the presence of guanidine and amidine in nafamostat, this compound is more easily ionized in the ESI positive mode than in the negative mode. Under the current condition, the most intense ions are the double-charged $[(M+2H)/2]^+$ in the positive mode, and $[M-H]^-$ in the negative mode, which confirms Yan-guang Cao's results [12]. In the ESI positive mode, *m/z* 174 from $[(M+2H)/2]^+$ was detected as the most intense ion, with an ion abundance of 100%, and *m/z* 348 from $[M+H]^+$ was also detected at 53.7% abundance. In the MS^2 spectrum, *m/z* 166 and 145 were obtained from the cleaving of *m/z* 174, and *m/z* 187 and 162 from *m/*

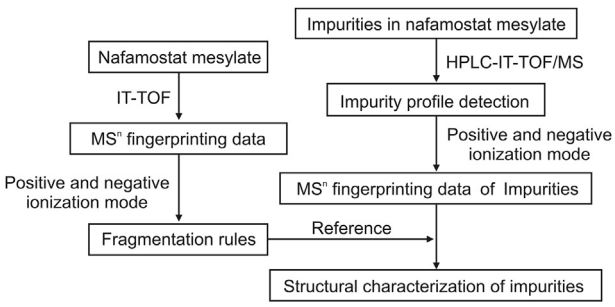

Fig. 2. Workflow of impurity identification in nafamostat mesylate.

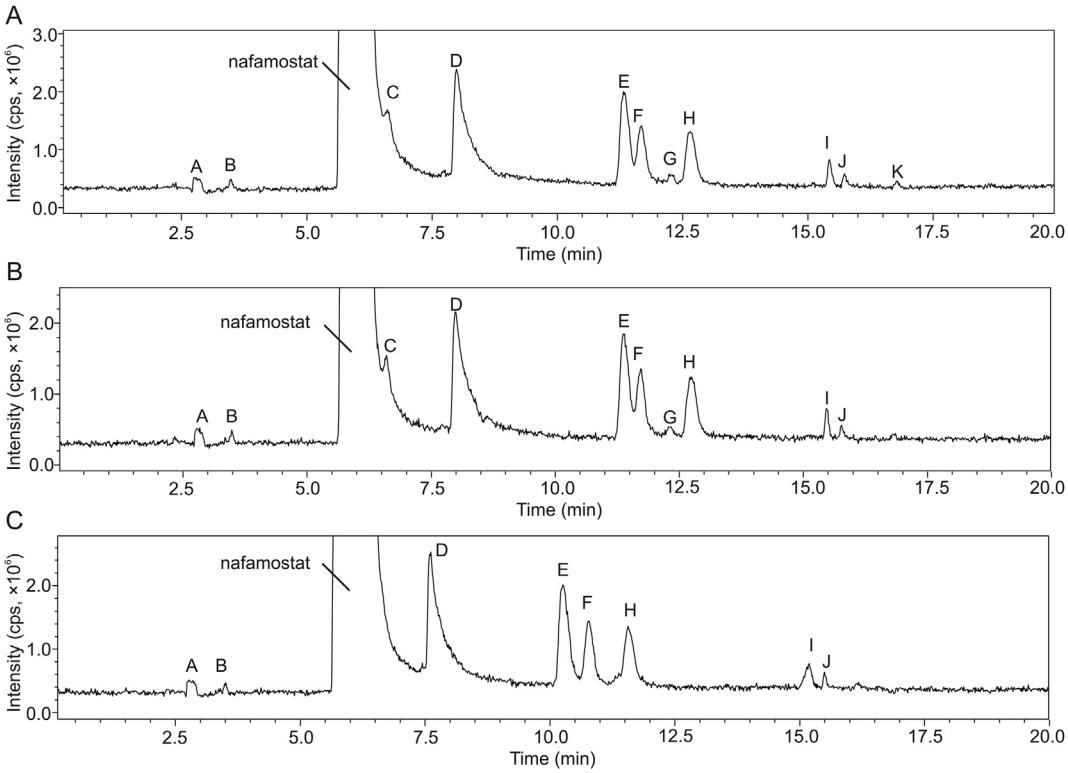

Fig. 3. Chromatograms of three batches of nafamostat mesylate. (A) Batch No:14092001, (B) Batch No:14092002, and (C) Batch No:14092003.

Table 1
IT-TOF MS^n analysis of nafamostat mesylate.

Ionization mode	MS_n	Observed mass (*m/z*)[a]	Proposed formula[a]	Calculated mass (*m/z*)[a]	Difference (ppm)	Ion abundance (%)
Positive	MS	348.1435 (1)	$C_{19}H_{18}N_5O_2^+$	348.1455 (1)	−5.74	53.7
		174.576 (2)	$C_{19}H_{19}N_5O_2^{2+}$	174.5764 (2)	−2.29	100
	MS^2	162.0660 (1)	$C_8H_8N_3O^+$	162.0662 (1)	−1.23	100
		187.0871 (1)	$C_{11}H_{11}N_2O_2^+$	187.0866 (1)	2.67	51.4
		166.0625 (2)	$C_{19}H_{16}N_4O_2^{2+}$	166.0631 (2)	−3.61	5.82
		145.0515 (2)	$C_{18}H_{14}N_2O_2^{2+}$	145.0522 (2)	−4.83	4.35
	MS^3	120.0435 (1)	$C_7H_6NO^+$	120.0444 (1)	−7.50	100
		170.0605 (1)	$C_{11}H_8NO^+$	170.0600 (1)	2.94	89.5
		157.5500 (2)	$C_{19}H_{13}N_3O_2^{2+}$	157.5498 (2)	1.27	25.7
Negative	MS	346.1327 (1)	$C_{19}H_{16}N_5O_2^-$	346.1309 (1)	5.20	100
	MS^2	304.1100 (1)	$C_{18}H_{14}N_3O_2^-$	304.1092 (1)	2.63	36.7
		185.0726 (1)	$C_{11}H_9N_2O^-$	185.0720 (1)	3.24	100
	MS^3	168.0482 (1)	$C_{11}H_6NO^-$	168.0455 (1)	4.17	100
		143.0534 (1)	$C_{10}H_7O^-$	143.0502 (1)	1.40	15.7

[a] (1): Single-charged ion, (2):Double-charged ion.

z 348. In the MS^3 spectrum of *m/z* 174, a product ion at *m/z* 157 was observed. In addition, the ion at *m/z* 170 could be generated from the cleaving of *m/z* 187. In the ESI negative mode, $[M - H]^-$ with a *m/z* of 346 was detected as the most abundant ion, and product ions at *m/z* 185 and 304 were observed. In the MS^3 spectrum, *m/z* 168 and 143 were generated from *m/z* 185. In summary, these characteristic product ions in both ESI positive and negative modes could be used to identify the impurities. The proposed fragmentation pathways of nafamostat are shown in Fig. 4.

3.4. Identification of seven impurities in nafamostat mesylate

Impurities in the different batches of nafamostat mesylate were identified. The retention time, molecular weight, proposed formula and MS product ions of seven impurities (**A**-**B**, **D**-**F**, **H**-**I**) in nafamostat mesylate are shown in Table 2. The MS spectra of the seven impurities are shown in Figs. S1- S7 and their structures in Fig. 5.

The most intense ions in the MS spectra of impurities **A** and **B** were not double-charged, which indicated that they could have been generated from the breaking of the ester bond. Nafamostat mesylate is synthesized from 4-guanidinobenzoic acid and 6-amidino-2-naphthol, and has one aliphatic amine group on each end, which is easily protonized. As a result, nafamostat mesylate has two ionization sites with high pka values. The molecular weights of impurities **A** and **B** were identified as 179 and 186, respectively, based on the ESI positive and negative modes, which correspond to 4-guanidinobenzoic acid and 6-amidino-2-naphthol. This was also validated by analyzing the standards of these two compounds.

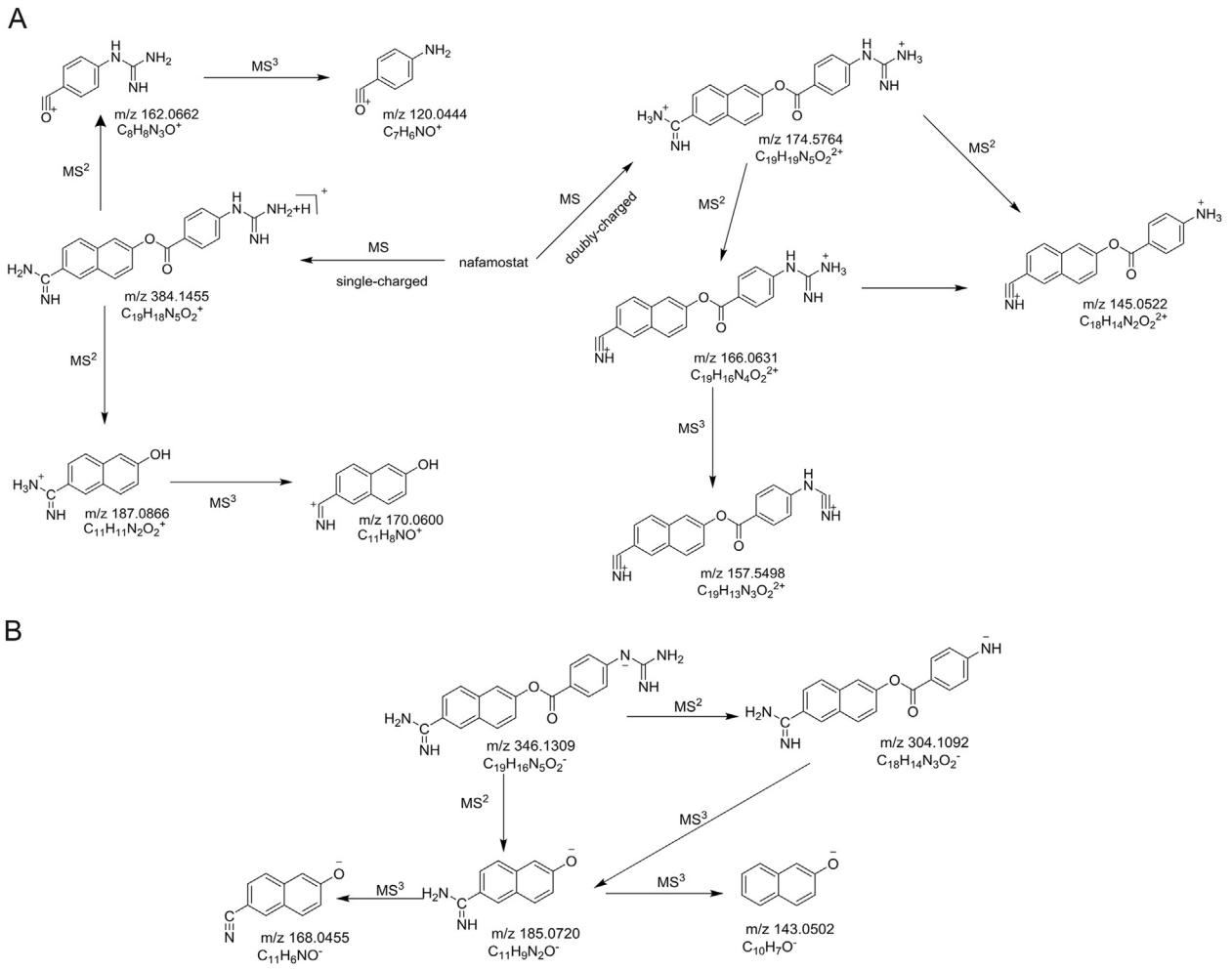

Fig. 4. Proposed fragmentation pathways of nafamostat. (A) Positive ionization mode and (B) negative ionization mode.

Table 2
Mass data of the impurities detected in nafamostat mesylate.

Impurity	t_R (min)	Molecular weight	Proposed formula	ESI positive mode MS_n[a]	ESI negative mode MS_n
A	2.96	179	$C_{11}H_{10}N_2$	MS:180; MS^2:162,120	MS:178;
B	4.67	186	$C_8H_9N_3O_2$	MS:187; MS^2:170	MS:185;
D	8.00	508	$C_{27}H_{24}N_8O_3$	MS:255 (2),509; MS^2:492,204,162,306,246 (2) MS^3:331,179,187,162,120,238 (2) MS^4:170,187,145	MS:507; MS^2:329,168,185,202 MS^3:168,185,143
E	11.35	509	$C_{27}H_{23}N_7O_4$	MS:256 (2),510; MS^2:180,163,161,144,331,120 MS^3:163,138	MS:508
F	11.67	348	$C_{19}H_{16}N_4O_3$	MS:349; MS^2:171,315,162,120 MS^3:143	MS:347; MS^2:305,186
H	12.65	466	$C_{26}H_{22}N_6O_3$	MS:234 (2),467; MS^2:225 (2),264,145,281,162,187 MS^3:170,120,145	MS:465; MS^2:185,168
I	15.45	305	$C_{18}H_{15}N_3O_2$	MS:306; MS^2:187,120,170	

[a] (2):Double-charged ion.

The most intense ions of impurities **D**, **E** and **H** in the MS spectra were double-charged, which suggests that these ions have at least two sites easily ionized in the ESI positive mode. Since these impurities have similar product-ion fragments at MS^2 and MS^3, they may have a structure similar to that of nafamostat. *m/z* 187 and 170 were observed as product-ion fragments of these impurities, which indicated that some 6-amidino-2-naphthol did not change. These three impurities were generated from 6-amidino-2-naphthol and 4-guanidinobenzoic acid. The molecular weight of impurity **D** was detected at 160Da higher than that of nafamostat, which indicated that it has a structure similar to that of 4-guanidinobenzoic acid. The structure characterization of impurity **D** was inferred from its ion fragmentation data. As the molecular weight of impurity **E** is only 1Da greater than that of impurity **D**, and a similar fragmentation pathway was identified for impurity **D**, we speculate that an N atom was substituted by an O. Fragments of impurity **H** were observed at *m/z* 162 and 120, which indicates that the part of 4-guanidinobenzoic acid was also present in this impurity. Meanwhile, the molecular weight of impurity **H** was detected at 119Da higher than that of nafamostat, from which we can deduce that

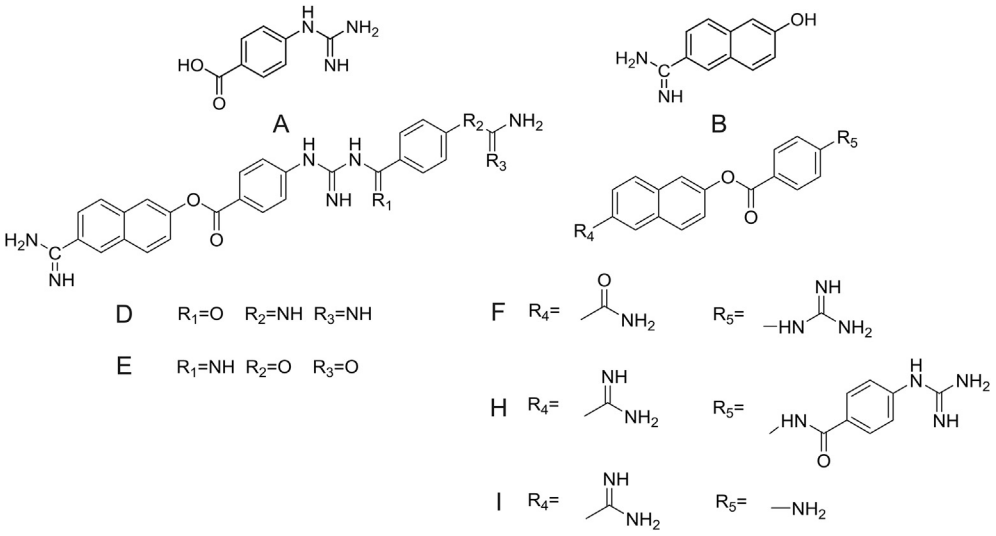

Fig. 5. Structures of seven impurities in nafamostat mesylate.

there may be a structure similar to that of the fragment ion at *m/z* 120. The structure of impurity **H** was characteristic of its fingerprint data.

The double-charged ions were not found in the MS spectra of impurities **F** and **I**, which suggests that only one easily-ionized site is present in their structure. Meanwhile, the molecular weight of impurity **F** is only 1Da higher than that of nafamostat according to those of the most intense ions in the positive and negative modes. We deduce that an N atom of the guanidine or amidino in nafamostat was substituted by an O atom to make impurity **F**. *m/z* 162 and 120 were detected among **F**'s ion fragments, indicating that the part of 4-guanidine benzoic acid did not change. Therefore, we deduce that an N atom in amidino was substituted. The structure of impurity **F** was identified from *m/z* 171 and 315. The molecular weight range of impurity **I**'s ion fragments in the negative ionization mode was lower than that in the positive mode, but the ion fragmentation information from the positive mode was consistent with the fragments of impurity **D**, and the structure of impurity **I** was identified accordingly.

4. Conclusions

The present work introduces an optimized HPLC-IT-TOF/MS method for detecting impurities in the nafamostat mesylate API. A reversed-phase LC method was developed to separate and detect eleven impurities. The impurities in nafamostat mesylate were characterized based on their fragmentation pathways and determined accurate molecular masses. In total, seven of the impurities were identified, which had not been previously reported. The results suggest that HPLC-IT-TOF/MS can be a useful and important method for the identification of impurities in drugs. This systematic study on impurity identification in nafamostat mesylate will help provide technical support in its quality control and clinical safety.

Conflicts of interest

The authors declare that there are no conflicts of interest.

Acknowledgments

This work was financially supported by the National Major Science and Technology Projects of China (2017ZX09101001) and the Double First-Class University Project (CPU2018GY33).

Appendix A. Supplementary data

Supplementary data to this article can be found online at https://doi.org/10.1016/j.jpha.2020.03.002.

References

[1] S. Mori, Y. Itoh, R. Shinohata, et al., Nafamostat mesilate is an extremely potent inhibitor of human tryptase, J. Pharmacol. Sci. 92 (2003) 420–423.
[2] M. Dobosz, Z. Sledzinski, P. Juszkiewicz, et al., Beneficial effect of therapeutic infusion of nafamostat mesilate (FUT-175) on hemodynamics in experimental acute pancreatitis, Hepatoik-Gastroenterology 38 (1991) 139–142.
[3] M. Piascik, G. Rydzewska, J. Milewski, et al., The results of severe acute pancreatitis treatment with continuous regional arterial infusion of protease inhibitor and antibiotic: a randomized controlled study, Pancreas 39 (2010) 863–867.
[4] Y. Koshiyama, A. Kobori, M. Ogihara, et al., The effects of FUT-175 (nafamostat mesilate) on blood coagulation and experimental disseminated intravascular coagulation (DIC), Nihon yakurigaku zasshi, Folia Pharmacol. Jpn. 90 (1987) 313–320.
[5] M. Uchiba, K. Okajima, H. Abe, et al., Effect of nafamostat mesilate, a synthetic protease inhibitor, on tissue factor-factor VIIa complex activity, Thromb. Res. 74 (1994) 155–161.
[6] K. Okajima, M. Uchiba, K. Murakami, Nafamostat mesylate, cardiovasc, Drug. Rev. 13 (1995) 51–65.
[7] C.W. Choi, D.H. Kang, G.H. Kim, et al., Nafamostat mesylate in the prevention of post-ERCP pancreatitis and risk factors for post-ERCP pancreatitis, Gastrointest. Endosc. 69 (2009) e11–e18.
[8] Y. Ohtake, H. Hirasawa, T. Sugai, et al., Nafamostat mesylate as anticoagulant in continuous hemofiltration and continuous hemodiafiltration, Contrib, Nephrology 93 (1991) 215–217.
[9] K. Kono, I. Tatara, S. Takeda, et al., Nafamostat mesylate therapy for systemic lupus erythematosus with nephrotic syndrome: a case report, Curr. Ther. Res. 57 (1996) 438–444.
[10] H. Schwertz, J.M. Carter, M. Russ, et al., Serine protease inhibitor nafamostat given before reperfusion reduces inflammatory myocardial injury by complement and neutrophil inhibition, J. Cardiovasc. Pharmacol. 52 (2008) 151–160.
[11] Q. Li, Y. Sai, Y. Kato, et al., Transporter-mediated renal handling of nafamostat mesilate, J. Pharmacol. Sci. 93 (2004) 262–272.
[12] Y.-G. Cao, M. Zhang, D. Yu, et al., A method for quantifying the unstable and highly polar drug nafamostat mesilate in human plasma with optimized solid-phase extraction and ESI-MS detection: more accurate evaluation for pharmacokinetic study, Anal. Bioanal. Chem. 391 (2008) 1063–1071.